EPS95 Ref. **eps0404**
Submitted to: **Pa-08**
Pl-11

Measurement of the semileptonic b branching ratios from inclusive leptons in Z decays.

The Aleph Collaboration

Abstract

From about 1.3 million hadronic Z decays collected with the ALEPH Detector in 1992 and 1993 inclusive muons and electrons have been analysed to measure the semileptonic branching ratios for primary and cascade b decays. The analyses take advantage of the high purity b sample obtained using lifetime tagging. A fit to the $p_\perp$ spectra gives the preliminary results

$$\begin{aligned} \mathrm{BR}(b \to \ell) &= 0.1101 \pm 0.0010_{\,\mathrm{stat}} \pm 0.0021_{\,\mathrm{syst}} {}^{+0.0024}_{-0.0017\,\mathrm{model}} \\ \mathrm{BR}(b \to c \to \ell) &= 0.0768 \pm 0.0018_{\,\mathrm{stat}} \pm 0.0031_{\,\mathrm{syst}} {}^{+0.0034}_{-0.0043\,\mathrm{model}} \end{aligned}$$

The model dependence has been reduced by using charge correlations in the event rather than fits to the $p_\perp$ spectra. A preliminary value of

$$\mathrm{BR}(b \to \ell) = 0.1101 \pm 0.0023_{\,\mathrm{stat}} \pm 0.0028_{\,\mathrm{syst}} \pm 0.0011_{\,\mathrm{model}}$$

has been obtained.

Contribution to the International Europhysics Conference on High Energy Physics
EPS–HEP Brussels, Belgium, 27 Jul.–2 Aug. 1995

1 Introduction

Three new measurements of inclusive semileptonic b branching ratios are presented, in which some of the main systematic uncertainties from previous analyses [1] have been reduced considerably [1].

Decays of the Z to b quarks can be selected with high efficiency and purity on the basis of the long b hadron lifetimes, using information from the silicon vertex detector [2]. This capability is exploited to prepare a pure b sample from which lepton candidates are selected. The events are divided in hemispheres with respect to the thrust axis. A probability for each track to come from the primary vertex is calculated based on its impact parameter. The probabilities from all tracks belonging to the same hemisphere are combined to give the probability (P_H) that the hemisphere contains no secondary vertices. A low value for P_H indicates the presence of a b quark.

The first analysis employs the yield of single lepton and same-side dilepton events, as well as the shape of the lepton spectra. This measurement is limited by the knowledge of the modelling of the $b \to \ell$ and $b \to c \to \ell$ spectra themselves. In a subsequent analysis the simultaneous fit of branching ratios and of the b fragmentation parameter allows part of the model dependence to be absorbed in the fragmentation uncertainty. In a third analysis, in which charge correlations are used in place of the $p_\perp$ spectra, some statistical power is sacrificed in order to obtain a measurement of $b \to \ell$ which is almost independent of modelling. The reduction in model dependence is also aided in the latter two analyses by reducing the momentum cut applied for electron identification.

In this paper the standard procedure for lepton spectra modelling, as agreed among the four LEP collaborations [3], is followed. The $b \to \ell$ spectrum is obtained by performing a fit to CLEO data of the ACCMM model. In order to estimate the systematic errors due to the modelling, two models are used as extremes: the GISW model, yielding harder spectra than the prediction of ACCMM, and the GISW**, yielding softer spectra due to an explicitly higher D^{**} contribution. The $c \to \ell$ spectrum is obtained by weighting the energy spectrum in the center of mass of the decaying charmed hadron, so that it reproduces the DELCO and MARK III data. The $b \to c \to \ell$ spectra are obtained by a two step process, combining $B \to D$, measured by CLEO, and $c \to \ell$ as described above.

The data sample consists of about 1.3 million hadronic decays of the Z collected by the ALEPH detector in the years 1992 and 1993. A description of the experimental apparatus and its performance can be found elsewhere [4, 5].

[1] The branching ratio to either electrons or muons (and not their sum), will be referred to as the semileptonic branching ratio.

2 Single lepton and same-side dilepton method

In this analysis the lifetime tagging is used to prepare a pure b sample by means of tracks belonging to one hemisphere, defined according to the thrust axis direction. Studying leptons in the opposite hemisphere allows BR($b \to \ell$) and BR($b \to c \to \ell$) to be measured. The lepton yield and spectra in hemispheres containing one lepton candidate or two opposite-charge lepton candidates are used. The details of the analysis can be found in Reference [6].

2.1 Measuring the b content of the selected sample

Leptons are selected following the criteria described in [7]. Only events with $|\cos\theta_{\rm thrust}| < 0.8$ are accepted. In order to extract the b semileptonic branching ratios, the fraction of the selected sample composed of $b\overline{b}$ events has to be known. It can be shown [2, 6] that the relevant parameter is $\varrho_b = \mathrm{R}_b \times \zeta_b$ where ζ_b is the efficiency for selecting b events with the lifetime tag at the cut considered.

The parameter ϱ_b is extracted from the fraction f_2 of double–tagged events in the data, using for R_b the latest LEP average [3]:

$$\begin{aligned} \mathrm{R}_b &= 0.2192 \pm 0.0018 \\ f_2 &= \frac{\varrho_b^2}{\mathrm{R}_b} + \lambda_b \left(\varrho_b - \frac{\varrho_b^2}{\mathrm{R}_b} \right) + \mathrm{R}_c \zeta_c^2 + (1 - \mathrm{R}_b - \mathrm{R}_c)\zeta_{uds}^2 \end{aligned}$$

where ζ_c and ζ_{uds} are the probabilities for selecting c or light quarks respectively; λ_b is the correlation between the b tagging probabilities in the two hemispheres.

The quantities ζ_c, ζ_{uds} and λ_b are estimated from the Monte Carlo simulation. A reweighting procedure is applied to charm events in the Monte Carlo, taking into account experimental measurements of charmed hadron lifetimes, production rates and topological branching ratios, as described in [8].

Using double–tagged events in order to measure ϱ_b brings in R_b as an additional source of systematics but on the other hand reduces the sensitivity to the charm and light quark efficiencies, which are estimated from the Monte Carlo.

2.2 The likelihood function

After applying the lifetime cut in one hemisphere, leptons are identified in the opposite hemisphere. Two subsamples are considered: hemispheres in which one lepton is found, and hemispheres in which two opposite–charge leptons are identified in the same jet. Since basically only b events can produce two prompt leptons in the same jet, the latter subsample has an intrinsically high purity, allowing a softer cut on the tagging side.

Schematically, the two subsamples are composed as follows:

$$\begin{aligned} N_1 &= N_{b\to\ell} + N_{b\to c\to\ell} + N_{bkg} \\ N_2 &= N_{b\to\ell,b\to c\to\ell} + N_{b\to\ell,bkg} + N_{b\to c\to\ell,bkg} + N_{bkg,bkg} \end{aligned}$$

For the two subsamples, beside the total number of expected hemispheres, the spectra of the single and dilepton samples are taken from the Monte Carlo simulation after applying a reweighting procedure and fitted to the data sample with the maximum likelihood method, leaving as free parameters the size of the $b \to \ell$ and $b \to c \to \ell$ contributions.

The likelihood function can therefore be written as the product of four separate contributions coming from the *counting* and from the *spectrum shape* of the two subsamples:

$$\begin{aligned} \mathcal{L} = & \frac{e^{-\mu_1}\mu_1^{N_1}}{N_1!} \times \prod_{i=1}^{N_1} \mathcal{F}_1(\mathrm{p}_\perp^i) \times & \text{(Single lepton)} \\ & \underbrace{\frac{e^{-\mu_2}\mu_2^{N_2}}{N_2!}}_{\text{Counting}} \times \underbrace{\prod_{j=1}^{N_2} \mathcal{F}_2(\mathrm{p}_{\perp 1}^j, \mathrm{p}_{\perp 2}^j)}_{\text{Spectra}} & \text{(Dileptons)} \end{aligned}$$

where μ_1, μ_2 are the number of hemispheres expected with one and two identified leptons respectively, and $\mathcal{F}_1$, $\mathcal{F}_2$ are the $\mathrm{p}_\perp$ distributions taken from the corrected Monte Carlo; they contain the two fitted parameters $\mathrm{BR}(b \to \ell)$ and $\mathrm{BR}(b \to c \to \ell)$; N_1, $\mathrm{p}_\perp^i$ and N_2, $(\mathrm{p}_{\perp 1}^j, \mathrm{p}_{\perp 2}^j)$ are the number of single leptons and dileptons in the data along with their measured $\mathrm{p}_\perp$ respectively.

The counting factors are affected by the uncertainty in the absolute efficiencies and have little dependence on the assumptions on the spectra shapes, while the opposite holds for the two spectral factors.

The contributions to the systematic error are evaluated moving each relevant parameter or spectrum by its estimated uncertainty (as described in Reference [6]), and performing again the fit. The optimization of the lifetime tag cut has been obtained by minimizing the total error. Cuts are set at $\log P_H < -4$ for the single lepton sample and $\log P_H < -2$ for the dilepton sample. The resulting sample compositions are shown in Table 1, with the lifetime tag cut only and after requiring one or two tagged leptons in the opposite hemisphere.

The likelihood contours for the subsamples are shown in Figure 1. For the single lepton subsample the counting and the spectra contributions are shown separately. The counting part basically gives the sum of the two parameters, and therefore introduces a strong negative correlation between them. The spectral part instead is basically sensitive only to a relative change of the amount of $b \to \ell$ and $b \to c \to \ell$, since varying them at the same time leaves the shape of the $\mathrm{p}_\perp$ spectrum essentially unaltered (a slight change is caused by the presence of some

Cut	bottom fraction	charm fraction	light quark fraction
$\log P_H < -4$	0.968	0.028	0.004
$\log P_H < -4$ and one lepton	0.983	0.016	0.001
$\log P_H < -2$	0.830	0.116	0.044
$\log P_H < -2$ and two leptons	0.983	0.015	0.002

Table 1: Estimated sample composition for the two P_H cuts with and without the lepton requirement in the hemisphere opposite to the tagging side.

background). It therefore brings a large positive correlation. For the dilepton subsample, the counting part gives basically information on the product of the two branching fractions, while the spectral part has much less statistical power; therefore the contour is hyperbola–like.

When leptons are selected in both hemispheres of an event, the event is considered twice, and in case both hemispheres fulfil the lifetime tag cut, two entries are used. This ensures that no bias is introduced in the average lepton content of the tagging side. Nonetheless some bias in the lifetime tag efficiency can be produced by the request of a lepton on the opposite side. The effect is investigated with the Monte Carlo simulation, and taken into account when extracting the branching ratios. Half of the effect is used as the uncertainty.

2.3 Results

The results of the fit are:

$$\begin{aligned} \mathrm{BR}(b \to \ell) &= 0.1134 \pm 0.0013_{\,\mathrm{stat}} \pm 0.0027_{\,\mathrm{syst}}\, {}^{+0.0041}_{-0.0027\ \mathrm{model}} \\ \mathrm{BR}(b \to c \to \ell) &= 0.0786 \pm 0.0019_{\,\mathrm{stat}}\, {}^{+0.0046}_{-0.0036\ \mathrm{syst}}\, {}^{+0.0039}_{-0.0047\ \mathrm{model}} \end{aligned}$$

The details of the systematic uncertainties are given in Table 2.

The statistical correlation coefficient between the two values is -0.44. It is basically due to the fact that the counting part of the likelihood has a greater statistical power than the spectrum shape part.

The main uncertainty comes from the knowledge of the lepton energy spectrum in the b or c hadron rest frame. This uncertainty mainly enters the part of the likelihood function concerning the $p_\perp$ shape of the single leptons, while the counting of lepton candidates is affected mostly by the unknowns in the background estimate.

Most of the systematic sources affect the relative ratio of lepton candidates which are interpreted as coming from direct or cascade decays. This induces a

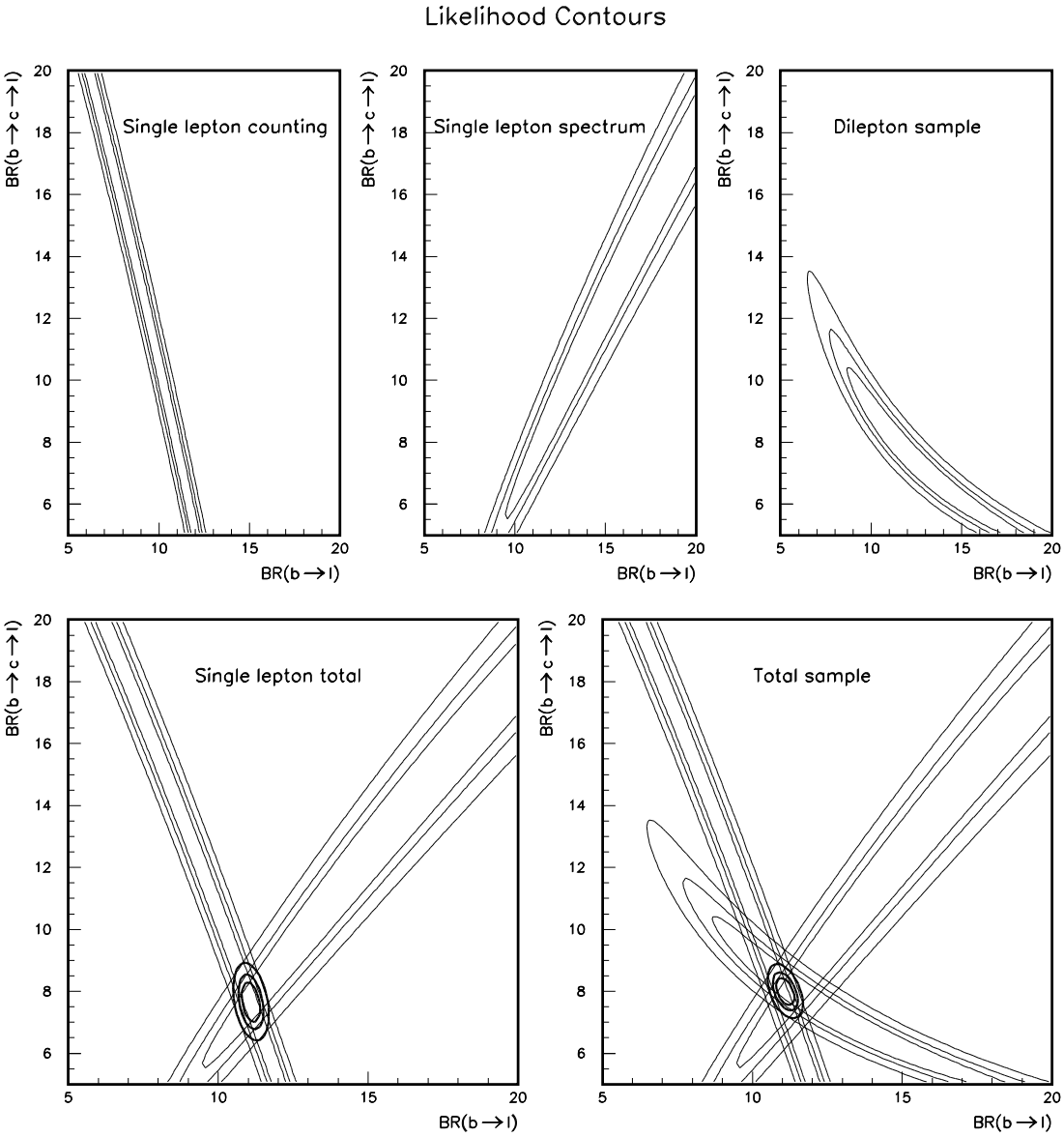

Figure 1: Likelihood contours corresponding to 1, 2 and 3σ for the single lepton subsample (for which the counting and the spectra contributions are shown separately), for the dilepton subsample, and for the total sample.

Source	$\Delta[\mathrm{BR}(b \to \ell)]$	$\Delta[\mathrm{BR}(b \to c \to \ell)]$
R_b	∓ 0.049	∓ 0.028
R_c	< 0.001	± 0.002
$\mathrm{BR}(c \to \ell)$	< 0.001	∓ 0.015
$\mathrm{BR}(b \to \mathrm{W} \to c \to \ell)$	< 0.001	∓ 0.164
$\mathrm{BR}(b \to \tau)$	∓ 0.025	∓ 0.054
$\mathrm{BR}(b \to u)$	∓ 0.038	± 0.107
$\mathrm{BR}(b \to \mathrm{J}/\psi)$	∓ 0.011	∓ 0.017
ε_b	± 0.190	± 0.099
ε_c	< 0.001	± 0.002
electron ID efficiency	∓ 0.049	∓ 0.051
muon ID efficiency	∓ 0.067	∓ 0.077
photon conversions	± 0.002	∓ 0.043
electron background	∓ 0.002	∓ 0.041
punch–through	∓ 0.012	$^{-0.205}_{+0.310}$
decaying hadrons	∓ 0.003	$^{-0.137}_{+0.204}$
gluon splitting	∓ 0.015	∓ 0.031
uds tagging probability	< 0.001	∓ 0.001
c tagging probability	± 0.002	± 0.017
b tagging probability	∓ 0.091	∓ 0.031
$P_H - \ell$ correlation	∓ 0.120	∓ 0.073
TOTAL	± 0.266	$^{+0.461}_{-0.364}$
$b \to \ell$ model	$^{-0.263}_{+0.407}$	$^{+0.333}_{-0.434}$
$c \to \ell$ model	$^{-0.055}_{+0.048}$	$^{-0.179}_{+0.191}$
$b \to$D model	$^{+0.039}_{-0.045}$	$^{-0.037}_{+0.039}$
Modelling TOTAL	$^{+0.412}_{-0.272}$	$^{+0.386}_{-0.471}$

Table 2: Estimated contributions to the systematic uncertainty on $\mathrm{BR}(b \to \ell)$ and $\mathrm{BR}(b \to c \to \ell)$ in %. Modelling uncertainties are shown separately from the other sources.

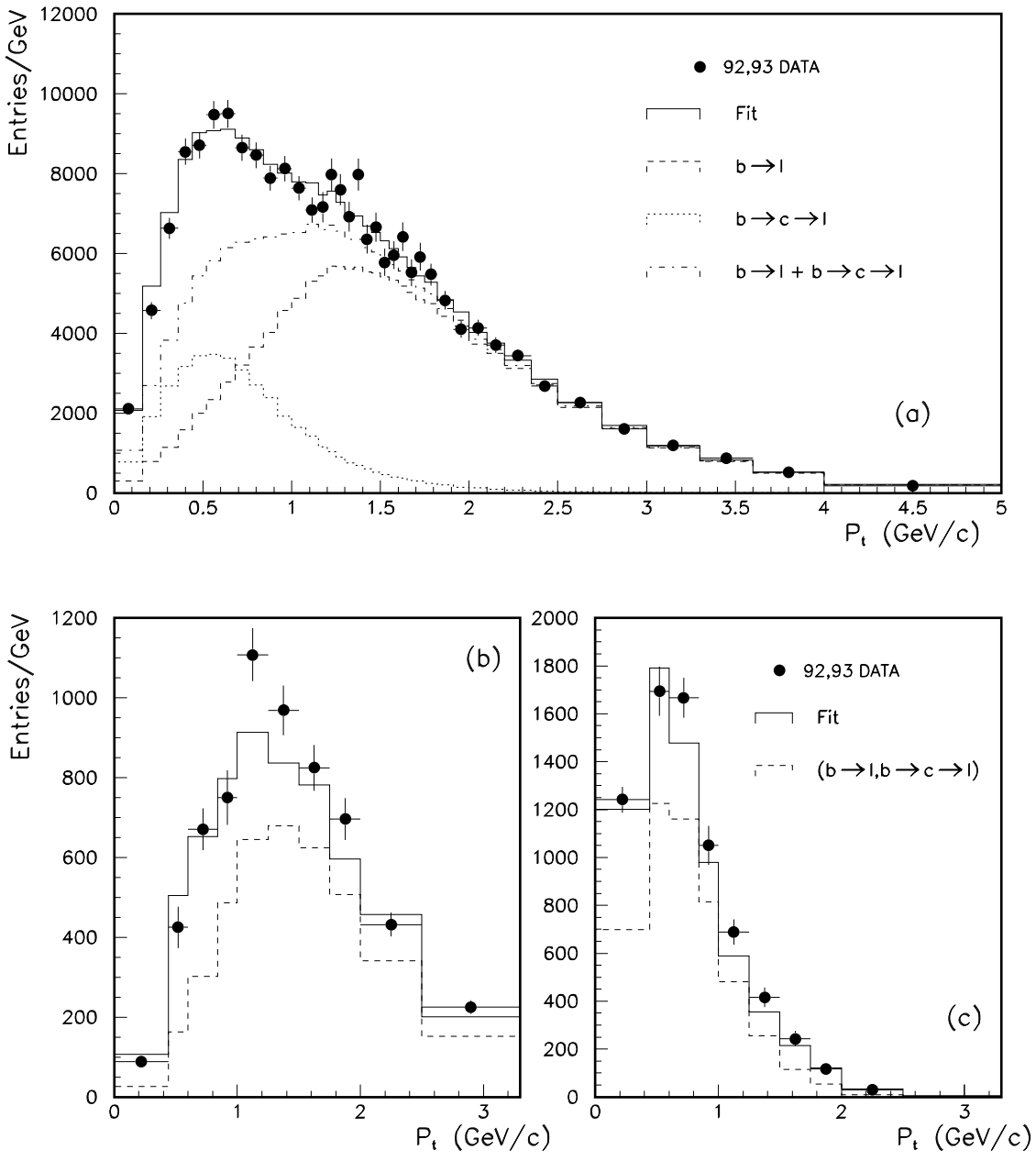

Figure 2: Comparison between measured spectra and fit results.
(a) Single lepton spectrum
(b) Dilepton sample: spectrum of the highest–$p_\perp$ lepton
(c) Dilepton sample: spectrum of the lowest–$p_\perp$ lepton
In (a) the contributions of the $b \to \ell$ and $b \to c \to \ell$ components (along with their sum) are also shown. In (b) and (c) the ($b \to \ell$,$b \to c \to \ell$) contribution is shown.

further negative correlation, so that the total correlation coefficient, taking into account both statistical and systematic errors, is -0.60.

In Figure 2 the $p_\perp$ spectra observed for the data are compared with the result of the fit showing a very good agreement over the entire $p_\perp$ range. The $b \to \ell$ and $b \to c \to \ell$ contributions are also shown for the single lepton sample, while the ($b \to \ell$,$b \to c \to \ell$) component is plotted for the dilepton sample.

3 Single lepton and opposite-side dilepton method

3.1 Introduction

An analysis has been performed that is similar to the previous one, but which allows the b hadron fragmentation parameter to vary in the fit. In this way advantage is taken of the partial cancellation between the systematic uncertainties from the $b \to \ell$ decay model and from the fragmentation.

The use of opposite-side dileptons rather than same-side dileptons increases the statistical power of the analysis. However, due to neutral B mixing, the average mixing parameter χ must also be fitted.

In principle there could be a difference in the extracted $b \to c \to \ell$ rate from same-side and opposite-side dileptons. A decay chain with two prompt leptons selects a sample of charm hadrons which may differ in composition from an unbiased sample (*i.e.* one in which the first W might decay to quarks), as the parent b hadron has decayed semileptonically. To avoid this effect, the same-side dileptons are not used in this fit.

Two subsamples are used:

- A sample of leptons coming from b decays has been selected with high purity thanks to the long lifetime of b hadrons. The primary b decays dominate the high (p,$p_\perp$) region, while the cascade decays fill the softer momenta region.
- The opposite-side dilepton sample is composed of pairs of leptons separated in the detector by an angle greater than $\pi/2$. Their charge correlation is taken into account in order to improve the statistical precision of the branching ratio measurement and to measure simultaneously the mixing parameter.

3.2 Data analysis

To help reduce the model dependence, the momentum cut for electron candidates is lowered from 3 GeV/c to 2 GeV/c in the present analysis. The identification efficiency is measured with the data as well as the main background coming from the converted photons, as a function of p and $p_\perp$. The muon candidates are required to have a momentum greater then 3 GeV/c. Their identification efficiency

is measured with the data; the contamination is determined from pure samples of hadrons, whilst the p and $p_\perp$ shapes are assumed from the Monte Carlo simulation [9].

3.2.1 The single lepton sample

A cut on the lifetime tag probability ($P_H < 10^{-4}$) was imposed on all hemispheres. For this cut the fraction of $b\overline{b}$ events is 96%, and the efficiency is 25%. The hemisphere opposite a tagged hemisphere is used as an unbiased sample of b decays. The lepton content of this sample is determined by computing the probability to identify a lepton as a function of p and $p_\perp$. This probability can be written in the following form, for its two main contributions:

$$\mathcal{P}(p, p_\perp) = \mathrm{BR}(b \to \ell)\mathcal{P}^{b\to\ell} + \mathrm{BR}(b \to c \to \ell)\mathcal{P}^{b\to c\to\ell} + \ldots$$

where $\mathcal{P}^{\mathrm{process}}$ is the probability to detect a lepton coming from a given process as a function of its p and $p_\perp$. $\mathcal{P}(p, p_\perp)$ does not depend, by construction, on either R_b or on the b tagging efficiency. The insensitivity of $\mathcal{P}(p, p_\perp)$ to R_b is an important new feature with respect to the previous measurements of $\mathrm{Br}(b \to \ell^-)$, since R_b and $\mathrm{Br}(b \to \ell^-)$ were strongly correlated in the published analysis [1]. If $\mathcal{P}^{b\to\ell}$ and $\mathcal{P}^{b\to c\to\ell}$ are known from elsewhere, a fit of $\mathcal{P}(p, p_\perp)$ allows $\mathrm{Br}(b \to \ell^-)$ and $\mathrm{Br}(b \to c \to \ell^+)$ to be determined.

Three efficiencies are needed for $\mathcal{P}^{\mathrm{process}}$:

$$\mathcal{P}^{\mathrm{process}} \propto \epsilon^{\mathrm{frag}}(\langle X_b \rangle) \times \epsilon^{\mathrm{model}}(E^*) \times \epsilon^{\mathrm{det}}(p, p_\perp)$$

where $\epsilon^{\mathrm{frag}}(\langle X_b \rangle)$ is the efficiency for a given $\langle X_b \rangle$ that a lepton passes the (p,$p_\perp$) cut, $\epsilon^{\mathrm{model}}(E^*)$ is the efficiency that a lepton with a given energy E^* in the center of mass of the b hadron passes the (p,$p_\perp$) cut, and $\epsilon^{\mathrm{det}}(p, p_\perp)$ is the efficiency to identify a lepton in the detector. The Peterson fragmentation scheme [10] is used to determine $\epsilon^{\mathrm{frag}}(\langle X_b \rangle)$ and the parameter ε_b of the Peterson function is left free in the fit to allow an adequate adjustment of this efficiency. Data are used to measure $\epsilon^{\mathrm{det}}(p, p_\perp)$. The determination of $\epsilon^{\mathrm{model}}(E^*)$ needs the knowledge of decay models for the different processes, which are taken from the lower energy data, as explained in the introduction.

The fit for $\langle X_b \rangle$, $\mathrm{Br}(b \to \ell^-)$ and $\mathrm{Br}(b \to c \to \ell^+)$ is performed over the full $p_\perp$ range.

3.2.2 The opposite-side dilepton sample

This sample is naturally enriched in b decays. It is used together with the single lepton sample to measure the semileptonic branching ratios and the mixing parameter χ, taking advantage of the charge correlations. The kinematical variables used to perform the fit on the dilepton sample are $p_\otimes = p_{\perp 1} \times p_{\|2} + p_{\perp 2} \times$

$p_{\|1}$ and $p_{\perp m}$ = Min($p_{\perp 1}$,$p_{\perp 2}$), where $\mathrm{p}_{\|i}$ and $\mathrm{p}_{\perp i}$ are respectively the longitudinal and transverse components of the lepton momentum with respect to the jet axis. They were found to be the most discriminating to separate $b \to \ell$ and $b \to c \to \ell$ processes [1].

3.3 Results

The main systematic uncertainties are summarised in Table 3.

The results, averaging over electrons and muons, are:

$$\begin{aligned} \mathrm{BR}(b \to \ell) &= 0.1101 \pm 0.0010_{\,\mathrm{stat}} \pm 0.0021_{\,\mathrm{syst}} \,{}^{+0.0024}_{-0.0017}{}_{\,\mathrm{model}} \\ \mathrm{BR}(b \to c \to \ell) &= 0.0768 \pm 0.0018_{\,\mathrm{stat}} \pm 0.0031_{\,\mathrm{syst}} \,{}^{+0.0034}_{-0.0043}{}_{\,\mathrm{model}} \end{aligned}$$

The values obtained for the other free parameters in the fit correspond to $\chi = (12.61 \pm 0.79)\%$ and $\langle X_b \rangle = 0.707 \pm 0.004$, in agreement with the previous ALEPH publication [1] and the current world averages (statistical errors only are quoted). The statistical correlation matrix from the fit is reported in Table 4. Figure 3 shows the results of the fit separated into the different planes which were used, and as a function of the charge of the dilepton pair.

This new analysis provides some significant improvements concerning systematic uncertainties. The use of a very pure sample of b events suppresses the charm and light quark contributions, and the quantity $\mathcal{P}(p, p_\perp)$ is constructed so as to render it independent of R_b.

4 Charge correlation method

4.1 Method

The measurements of semileptonic branching ratios described in the previous sections utilize fits of $\mathrm{p}_\perp$ distributions to extract the branching ratios, and thus retain significant model dependence. Another method, described here, uses no prediction for the $\mathrm{p}_\perp$ spectra, yet still attains an interesting statistical precision.

The main problem in measuring BR($b \to \ell$) lies in differentiating the contributions from *direct* decays ($\mathsf{B} : b \to c\ell^-\nu$) and from *cascade* decays ($\mathsf{C} : b \to c \to s\ell^+\nu$). Direct and cascade leptons can be distinguished based on the correlation of their charge with that of the b quark, a fact used in this method in place of the information carried by the $\mathrm{p}_\perp$ distributions.

Although physics interest lies mainly with BR($b \to \ell$) ($\equiv \mathsf{B}$), in fact both B and C must be measured simultaneously. Two independent measurements are needed to separate them. The fraction of b hadrons producing one prompt lepton (F_1), and the fraction of opposite-side dilepton events in which the leptons have opposite charge (F_{OS}), have been chosen. In the ideal case (*i.e.* neglecting

Source	Var.	$b \to l$	$b \to c \to l$
$b \to l$ model		$^{+0.22}_{-0.12}$	$^{-0.40}_{+0.32}$
$B \to D$ model		$^{-0.04}_{+0.04}$	$^{+0.06}_{-0.06}$
$c \to l$ model		$^{+0.09}_{-0.12}$	$^{+0.10}_{-0.15}$
Total model		$^{+0.24}_{-0.17}$	$^{+0.34}_{-0.43}$
Electron ID efficiency	2 %	0.12	0.13
photon conversions	10 %	0.02	0.08
electron background	10 %	-	0.02
Total electron		0.12	0.15
Muon ID efficiency	2 %	0.11	0.07
decaying hadrons	10 %	0.01	0.07
punch–through	20 %	0.01	0.16
punch + decays shape		0.08	0.03
Total muon		0.14	0.19
$b \to \psi$	14 %	0.02	0.01
$b \to \tau$	18 %	0.04	0.06
$b \to W$	20 %	0.01	0.14
$b \to u$	50 %	0.03	0.09
Total Br		0.05	0.18
$udsc$ impurity		0.08	0.04
back. charge asym.		0.02	0.05
TOTAL syst		$^{0.32}_{0.27}$	$^{0.46}_{0.53}$
TOTAL stat		0.10	0.18
TOTAL		$^{0.33}_{0.28}$	$^{0.49}_{0.56}$

Table 3: Table of systematics for the measurements of the branching ratios.

ρ	$b \to l$	$b \to c \to l$	$\langle X_b \rangle$	χ
$b \to l$		- 0.37	- 0.63	0.13
$b \to c \to l$			0.03	- 0.18
$\langle X_b \rangle$				- 0.06

Table 4: Statistical correlation matrix between $b \to l$, $b \to c \to l$, $\langle X_b \rangle$ and χ.

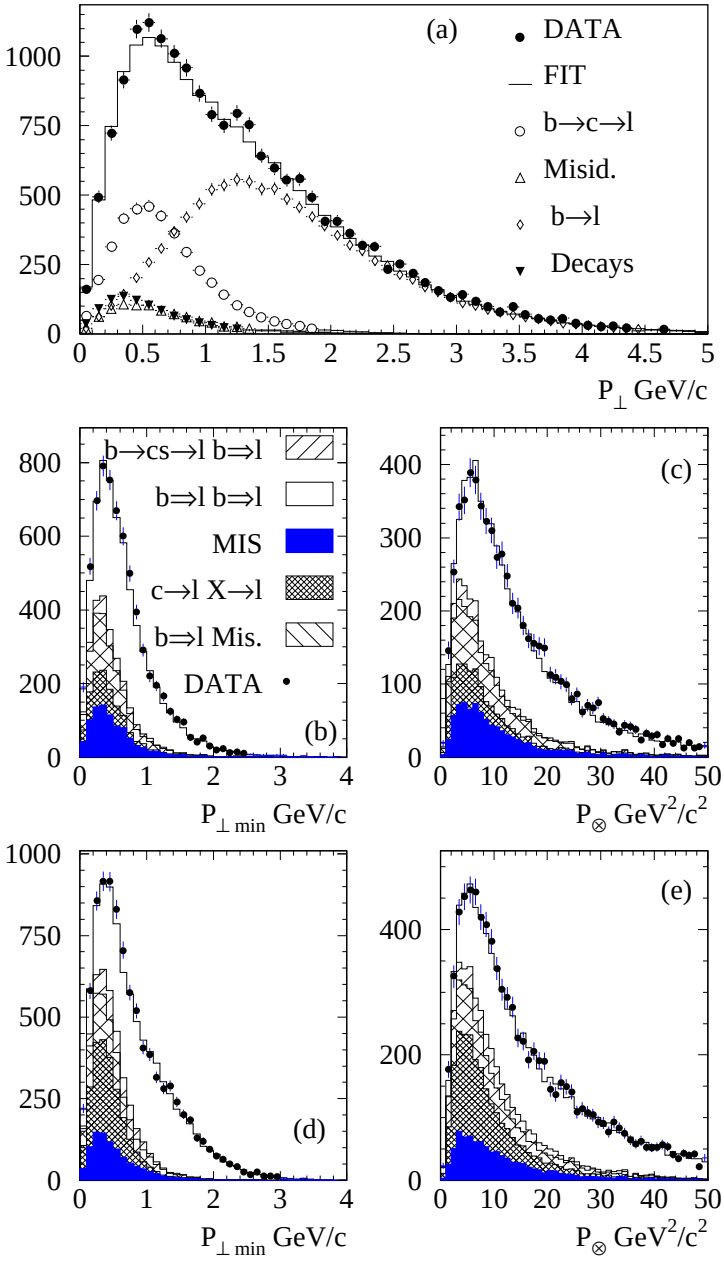

Figure 3: (a) result of the fit to the single lepton sample enhanced in b events, (b) result of the fit to $p_{\perp m}$ for opposite-side, same-sign dileptons, (c) result of the fit to $p_{\otimes}$ for opposite-side, same-sign dileptons, (d) result of the fit to $p_{\perp m}$ for opposite-side, opposite-sign dileptons, (e) result of the fit to $p_{\otimes}$ for opposite-side, opposite-sign dileptons. $b \Longrightarrow l$ represents $b \to X \to l$.

lepton identification efficiency, contamination, physics backgrounds, mixing and mistagging) the observed quantities would be

$$F_1 = \mathsf{B}(1-\mathsf{C}) + (1-\mathsf{B})\mathsf{C} \ , \qquad F_{\rm OS} = \frac{\mathsf{B}(1-\mathsf{C})}{\mathsf{B}(1-\mathsf{C}) + (1-\mathsf{B})\mathsf{C}}$$

which easily can be seen to separate B and C. In reality, lepton selection efficiency, lepton contamination, the average rate of neutral B mixing, and physics backgrounds (such as $\mathrm{b} \to \overline{\mathrm{c}}s \to \ell^-$, $\mathrm{b} \to \tau \to \ell^-$, and $\mathrm{b} \to \psi, \psi'$) must all be taken into account.

The observed values for F_1 and $F_{\rm OS}$ come from two different samples of events.

- The single-lepton fraction (F_1) is the fraction of lifetime-tagged hemispheres in which exactly one lepton (electron or muon) is found. A severe tagging requirement ($P_H < 10^{-6}$) is applied, giving a $\mathrm{b\overline{b}}$ purity above 98% (higher when a lepton is observed), so systematics from $\mathrm{c\overline{c}}$ contamination are very small. The important systematics coming from the lepton selection have received special attention, as described below.

- The opposite-sign fraction ($F_{\rm OS}$) separates the contributions B and C to F_1. This sample of opposite-side dilepton events is almost independent of the single-lepton sample selected using the lifetime tag. The *tag* lepton is required to have a large $\mathrm{p}_\perp$ (> 1 GeV/c) so that its charge accurately reflects the charge of the decaying b quark [2]. The *signal* lepton satisfies exactly the same criteria as those in the single-lepton sample. The decaying b quark sometimes has charge opposite that of the produced b quark, due to neutral B meson mixing. The average rate of mixing, measured by several collaborations, is used [11]. The mistag rate, measured from the data, is about 17%. The systematics coming from lepton selection are reduced for $F_{\rm OS}$ since it is a ratio. The tagging requirement was chosen to reduce the $\mathrm{c\overline{c}}$ contamination to only 4%, for which the systematics are evaluated using a tagged $\mathrm{c\overline{c}}$ sample from the data.

  In order to compensate the statistical dilution of $F_{\rm OS}$ caused by the mistagging and neutral B mixing, the dilepton sample was augmented by a sample of single leptons opposite a hemisphere passing a tight jet-charge cut. The jet charge is calculated with all charged tracks in a hemisphere, using rapidity (with respect to the thrust axis) as a weight. A soft lifetime-tag requirement ($P_H < 2 \times 10^{-4}$) is applied to the same hemisphere to suppress $\mathrm{c\overline{c}}$ events. The cuts on jet charge and P_H were chosen to match the performance of the high-$\mathrm{p}_\perp$ lepton tag: the mistag rate is 20% and the $\mathrm{c\overline{c}}$ contamination

[2] The $\mathrm{p}_\perp$ is calculated including the lepton in the definition of the jet momentum, in contrast to the other two analyses. The tag lepton charge correctly reflects the charge of the decaying b quark 90% of the time.

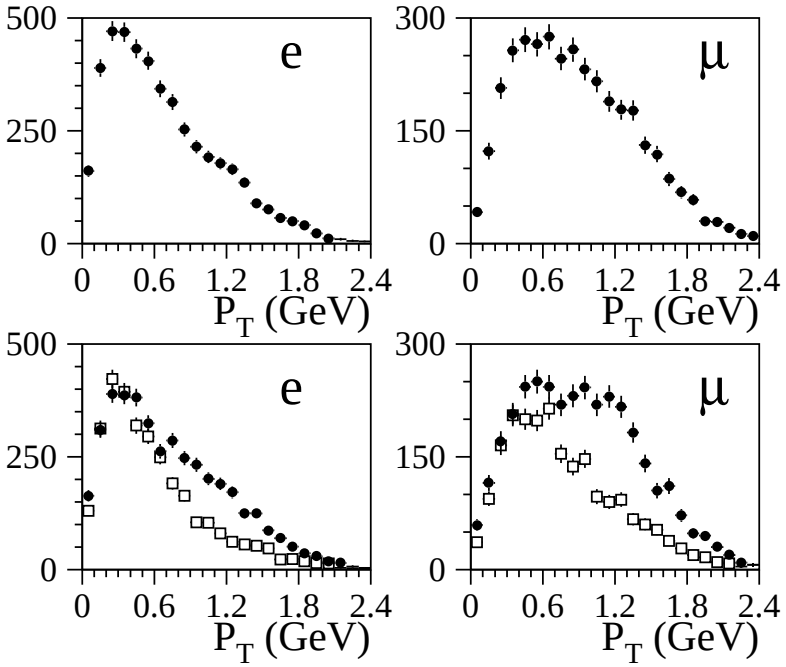

Figure 4: Raw $p_\perp$ distributions, for electrons and muons separately. The upper plots show leptons selected opposite a lifetime tag. The lower plots show leptons opposite either a high-$p_\perp$ lepton, or a hemisphere passing the jet charge requirement. The filled dots represent opposite-sign leptons, and the open squares, same-sign.

4%. The jet-charge sample is constructed to be strictly independent of the dilepton sample, and its overlap with the single-lepton sample is less than 5%. It improves the statistical precision of $\mathrm{BR}(b \to \ell)$ by 20%.

The method sketched above differentiates leptons based on their charge only. Consequently, the quantity B includes 'direct' leptons from $\mathrm{b} \to \mathrm{W}^- \to \ell^-$ as well as 'secondary' leptons $\mathrm{b} \to \mathrm{W}^- \to \overline{c}s, \tau^- \to \ell^-$. The acceptance for secondary leptons is taken from the simulation, but the rates are based on measurements. The production of ψ,ψ' and $b \to u$ transitions also are taken into account.

4.2 Results

The raw $p_\perp$ distributions for the single-lepton and dilepton samples are displayed in Figure 4. The dilepton distribution is divided into the opposite-sign and same-sign pieces, and includes the events tagged with jet charge (40% of the total). Taking electrons and muons together, there are 8002 single leptons (*i.e.* opposite a lifetime tag), 4554 opposite-sign and 3091 same-sign dileptons.

The semileptonic branching ratios are derived separately for electrons and muons and for the two different years of running. The values are combined to give

$$\mathrm{BR}(b \to \ell) = 0.1101 \pm 0.0023 \qquad \text{and} \qquad \mathrm{BR}(b \to c \to \ell) = 0.0830 \pm 0.0031.$$

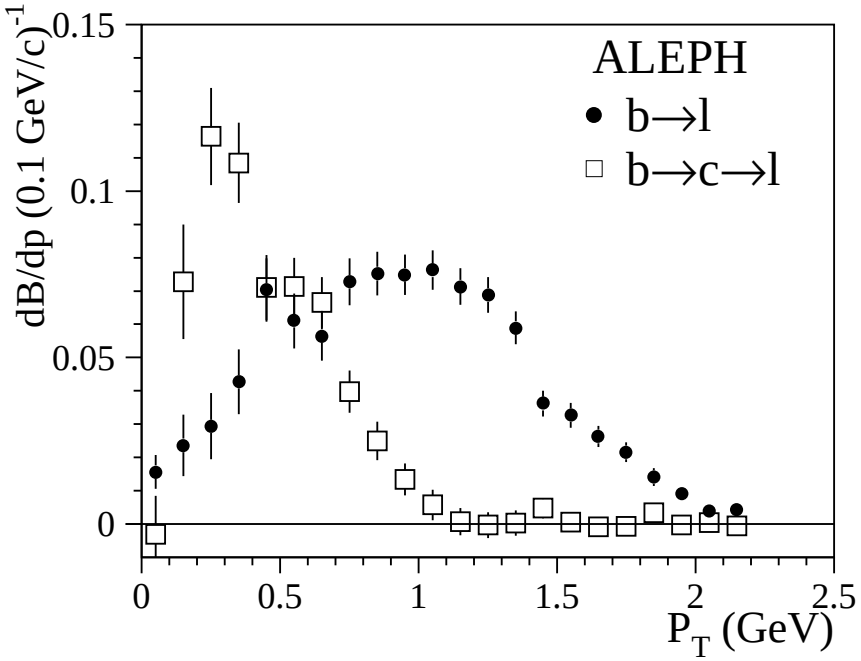

Figure 5: Derived $p_\perp$ distributions, for $b \to \ell$ represented by the filled circles, and for $b \to c \to \ell$ represented by the open squares.

The correlation coefficient is -0.4. The analysis can be performed in bins of $p_\perp$ with the result shown in Figure 5.

Since the sum of B and C is given mainly by F_1 which depends strongly on the lepton acceptance, a new selection technique has been developed to reduce systematic uncertainties [12]. In a first step, tracks are selected if they pass simple geometric requirements for which the simulation is very reliable. Weaker regions of the detector are avoided. For the second step, the standard electron and muon estimators [7] are combined in two global variables (η_e and η_μ) which, by construction, are distributed uniformly between zero and one for electrons and muons. Hadrons are concentrated near η_e, $\eta_\mu = 0$, so a cut on η_e or η_μ removes them while retaining a known fraction of electrons or muons. With this technique, the uncertainty for the lepton selection is reduced by a factor of two with respect to Ref. [1].

The acceptance for the momentum requirement is calculated using the simulation. The result depends slightly on the model of the lepton energy spectrum in the b hadron rest frame. For electrons, the minimum momentum requirement is $p > 1$ GeV/c, for which the acceptance is 92.9%. This acceptance changes by 0.32% as the two extreme models are considered, leading to an uncertainty in BR($b \to \ell$) of 0.065%. For muons the cut is higher (3 GeV/c), leading to a smaller acceptance (78.0%) and larger branching ratio uncertainty (0.170%). The branch-

source of uncertainty	$\Delta\mathrm{BR}(b \to \ell)$	$\Delta\mathrm{BR}(b \to c \to \ell)$
lepton selection	0.112	0.143
lepton contamination	0.063	0.102
b hadron fragmentation	0.073	0.224
mistag	0.107	0.214
mixing	0.090	0.155
single-lepton b-purity	0.033	0.030
$c\overline{c}$ in dileptons & jet-charge	0.087	0.148
$b \to \overline{c}s \to \ell^-$	0.156	-
$b \to \tau \to \ell^-$	0.058	-
$b \to \psi, \psi'$	0.040	0.040
$b \to u$	-	0.042
subtotal	0.282	0.421
model dependence	0.112	0.116
total	0.303	0.437

Table 5: Summary of systematic uncertainties. All numbers are in percent.

ing ratio uncertainties for electrons and muons are combined linearly according to the number of electrons and muons, giving $\Delta\mathrm{BR} = 0.112\%$.

The individual sources of lepton contamination have been identified before [7]. They have been studied with new data, allowing more accurate corrections to the predictions taken from the simulation. For example, converted photons are selected from pairs of tracks of which at least one is a clean electron. Hadrons misidentified as muons are selected in events depleted of long-lived hadrons. The correction factors are close to one, with an uncertainty of 5%.

The uncertainty in the acceptance due to the momentum spectrum of the decaying b hadrons is taken into account using the measurement of the average energy fraction, $\langle X_b \rangle$, reported by ALEPH [13]. The Peterson fragmentation parameter in the simulation was varied to cover the full range of $\langle X_b \rangle$, giving a variation for the lepton acceptance due to the momentum requirement.

The b purity of the single lepton sample is obtained using the double-tag method [2]. Its uncertainty is propagated to the branching ratio. The Monte Carlo prediction for the $c\overline{c}$ contamination in the dilepton sample is checked using events tagged with a fast D or $D^\star$ meson. The uncertainty comes from the statistical precision of this test, which includes the value of F_{OS} for $c\overline{c}$ events.

The average mixing for b hadrons produced in Z decays, χ, is taken from the LEP average [11]. The mistag rate is measured directly with the data. Its statistical uncertainty is propagated to give systematic uncertainties for the branching ratios.

The corrections for secondary leptons (which must be subtracted from B to obtain the direct branching ratio), for B$\to \psi, \psi'$, and for $b \to u$ transitions are based on measurements made elsewhere [14].

A summary of all uncertainties is given in Table 5.

5 Conclusion

New methods for measuring the semileptonic branching ratios employing lifetime tagging have been presented. An analysis based on the fit of lepton spectra for single leptons and same-side dileptons gives

$$\begin{aligned} \mathrm{BR}(b \to \ell) &= 0.1134 \pm 0.0013_{\,\mathrm{stat}} \pm 0.0027_{\,\mathrm{syst}} \,^{+0.0041}_{-0.0027}{}_{\,\mathrm{model}} \\ \mathrm{BR}(b \to c \to \ell) &= 0.0786 \pm 0.0019_{\,\mathrm{stat}} \,^{+0.0046}_{-0.0036}{}_{\,\mathrm{syst}} \,^{+0.0039}_{-0.0047}{}_{\,\mathrm{model}} \end{aligned}$$

where 'syst' refers to the experimental systematic errors (including b hadron fragmentation), and 'model' refers to the uncertainty coming from the decay model.

In a subsequent analysis the simultaneous fit of branching ratios and of the b fragmentation parameter allows part of the model dependence to be absorbed in the fragmentation uncertainty, giving

$$\begin{aligned} \mathrm{BR}(b \to \ell) &= 0.1101 \pm 0.0010_{\,\mathrm{stat}} \pm 0.0021_{\,\mathrm{syst}} \,^{+0.0024}_{-0.0017}{}_{\,\mathrm{model}} \\ \mathrm{BR}(b \to c \to \ell) &= 0.0768 \pm 0.0018_{\,\mathrm{stat}} \pm 0.0031_{\,\mathrm{syst}} \,^{+0.0034}_{-0.0043}{}_{\,\mathrm{model}} \quad . \end{aligned}$$

The model dependence has been further reduced at the cost of enlarging the statistical errors by using charge correlations in the event rather than fits to the $p_\perp$ spectra. The values obtained are

$$\begin{aligned} \mathrm{BR}(b \to \ell) &= 0.1101 \pm 0.0023_{\,\mathrm{stat}} \pm 0.0028_{\,\mathrm{syst}} \pm 0.0011_{\,\mathrm{model}} \\ \mathrm{BR}(b \to c \to \ell) &= 0.0830 \pm 0.0031_{\,\mathrm{stat}} \pm 0.0042_{\,\mathrm{syst}} \pm 0.0012_{\,\mathrm{model}} \quad . \end{aligned}$$

The three set of results are consistent with each other and with previous results published by the ALEPH Collaboration [1]. These results are preliminary and cannot be simply averaged as they are correlated.

References

[1] ALEPH Coll., D. Buskulic *et al.* , Z. Phys. **C62** (1994) 179.

[2] ALEPH Coll., D. Buskulic *et al.* , Phys. Lett. **B313** (1993) 535.

[3] The LEP Electroweak Working Group, ALEPH / 94–119, (LEP note LEPHF 94–003) , 19 July 1994.

[4] ALEPH Coll., D. Decamp *et al.* , Nucl. Instr. Methods **A294** (1990) 121.

[5] ALEPH Coll., D. Buskulic *et al.* , Nucl. Instr. Methods **A360** (1995) 481.

[6] D. Abbaneo, F. Ligabue and N. Marinelli ALEPH / 95–071, 26 June 1995.

[7] ALEPH Coll., D. Buskulic *et al.* , Nucl. Instr. Methods **A346** (1994) 461.

[8] D. Brown *et al.* , ALEPH / 93–039, 2 March 1993;
D. Brown *et al.* , ALEPH / 93–083, 17 May 1993 .

[9] P.Perret and S.Monteil, ALEPH / 94–055, 19 April 1994.

[10] C. Peterson, et al., Phys. Rev. **D27** (1983) 105.

[11] The LEP Electroweak Working Group, CERN PPE/94-187.

[12] M.Schmitt, ALEPH / 95–005, 15 January 1995.

[13] ALEPH Coll., D. Buskulic *et al.* , *Measurement of the effective b quark fragmentation function at the Z^0 resonance*, submitted to Phys. Lett.

[14] Particle Data Group, "Review of Particle Properties," Phys. Rev. **D50** (1994).